Analyst

PAPER

Cite this: *Analyst*, 2015, **140**, 4245

A peptide nucleic acid-functionalized carbon nitride nanosheet as a probe for *in situ* monitoring of intracellular microRNA†

Xianjiu Liao, Quanbo Wang and Huangxian Ju*

Received 20th January 2015,
Accepted 17th April 2015

DOI: 10.1039/c5an00128e

www.rsc.org/analyst

A novel probe for recognition of both cancer cells and intracellular microRNA (miRNA) is designed by functionalizing a carbon nitride nanosheet (f-CNNS) with a Cy5-labeled peptide nucleic acid (Cy5-PNA) and folate. The interaction between Cy5-PNA and CNNS quenches the fluorescence of Cy5, and the presence of folate endows the probe with good specificity to folate acceptor overexpressed cells. The probe can be specifically taken up by cancer cells with an incubation step. Upon the recognition of the PNA to complementary miRNA, the hybridization product is released from the CNNS surface, which leads to the fluorescence recovery and provides a specific method for sensing of miRNA. Thus, this probe can be used for cell-specific intracellular miRNA sensing with a confocal microscope. Using miRNA-18a as a target model, the dynamic changes of its expression level inside living cells can be monitored with the proposed method. This method possesses promising applications in the study of miRNA related bioprocesses and biomedicine.

Introduction

MicroRNAs (miRNAs) are a group of evolutionally conserved, endogenously expressed, non-coding, small-sized and non-protein-coding RNAs. They play post-transcriptional regulatory roles in a wide variety of biological processes including early development, cellular differentiation, proliferation, and apoptosis.[1–4] Specifically, the aberrant expression and misregulation of miRNAs can lead to various diseases,[5–8] including human cancer.[9–11] Thus their expression profiles can be used as biomarkers for the onset of disease states, and it is possible to use miRNAs in gene therapy for genetic disorders as well as potential drug targets.[12–14] Many techniques such as real-time quantitative PCR,[15,16] northern blotting[17,18] and microarrays[19] have been extensively used for miRNA analysis. However, these techniques need a miRNA isolation step for sample preparation; the *in situ* monitoring of miRNAs in living cells is still a challenge owing to the unique characteristics of intracellular miRNA.

Benefiting from the development of new materials, our previous work proposed several systems for cellular delivery of recognition probes to monitor intracellular miRNA and telomerase.[20–23] Recently, bulk graphitic-phase carbon nitride ($g\text{-}C_3N_4$), a kind of metal-free semiconductor and a representative 2D layered nanomaterial analogous to graphene that has been extensively used in biological fields,[24–26] has drawn growing attention in the biosensing field due to its special structure, optical and electrical properties.[27–30] The carbon nitride nanosheet (CNNS) can be exfoliated from bulk $g\text{-}C_3N_4$ to directly disperse in aqueous solution.[31] This work used CNNS as a novel carrier to construct a probe (f-CNNS) for recognition of both cancer cells and miRNA and proposed a method for *in situ* monitoring of intracellular miRNA.

The recognition of the probe to miRNA was achieved with the loaded peptide nucleic acid (PNA), a non-natural nucleic acid analog. Its backbones are held together not by negatively charged-phosphodiester bonds as in DNA, but by the uncharged amide bonds.[32–35] As shown in Fig. 1A, the f-CNNS probe was prepared by assembling Cy5-labeled PNA (Cy5-PNA) and then folate (FA)-Poly A on CNNS through strong π–π interactions.[36,37] The loading of Cy5-PNA on CNNS led to the quenching of Cy5 fluorescence (FL) by CNNS,[32,36] and the presence of FA on CNNS achieved cell-target-specific delivery.[38,39] After the f-CNNS probe was transfected into the cells, the hybridization of the assembled Cy5-PNA with a complementary target weakened the π–π interaction between bases and CNNS, which led to the release of the Cy5-PNA from CNNS, and thus recovered the quenched FL (Fig. 1B). The recovered FL could specifically respond to the complementary target, leading to a strategy for sensing of miRNA in a living cell. The miRNA sensor allows high selectivity and specificity toward target

State Key Laboratory of Analytical Chemistry for Life Science, Department of Chemistry, Nanjing University, Nanjing 210093, PR China

†Electronic supplementary information (ESI) available. See DOI: 10.1039/c5an00128e

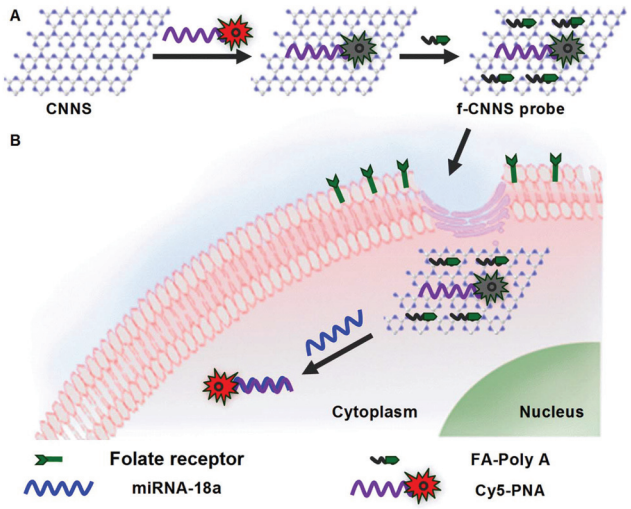

Fig. 1 Schematic illustration of (A) f-CNNS probe preparation and (B) detection of intracellular miRNA with the f-CNNS probe.

miRNA with a very low background signal, thus providing a powerful tool for the study of intracellular miRNA-related biological events.

Experimental

Materials and reagents

Carbon nanospheres (CNS) were prepared according to the literature.[40] HepG2, HeLa, A549, MDA-MB-231 and HaCaT cells, Annexin V-FITC, propidium iodide (PI), 3-(4,5-dimethylthiazol-2-yl)-2-diphenyltetrazolium bromide (MTT), and pH 7.4 binding buffer were from KeyGen Biotech. Co. Ltd (Nanjing, China). DNase I endonuclease was from Thermo Fisher Scientific Inc. (USA), and ssDNA binding protein (SSB) was from Promega Corporation (USA). Lipofectamine 2000 (Lp2000), serum-free medium (Opti-MEM), Hoechst 333342 as a nuclear tracker and LysoTracker Green DND-26 as an endosomal/lysosomal tracker were obtained from Invitrogen Corporation (USA). Graphene oxide was obtained from XFNano Materials Tech Co., Ltd (Nanjing, China). Folate (FA) and 2-mercaptoethanol were obtained from Sigma-Aldrich Inc. (USA). DNA hybridization buffer (HB) was Tris-HCl buffer (20 mM, containing 100 mM NaCl, 5.0 mM KCl, and 5.0 mM $MgCl_2$, pH 7.4). Ultrapure water obtained from a Millipore water purification system (≥18 MΩ, Milli-Q, Millipore) was used in all runs. All PNA, RNA, locked nucleic acid (LNA) and DNA sequences were purchased from Panagene, Inc. (Daejeon, Korea), Shanghai GenePharma Co., Ltd and Sangon Biological Engineering Technology Co., Ltd (Shanghai, China), respectively. Their sequences were listed as follows with mismatched and LNA modified bases in the italic type: miRNA-18a: 5′-UAAGGUGCAUCUAGUGCAGAUAG-3′; miRNA-18a mimic included miRNA-18a and its antisense sequence: 5′-AUCUGCACUAGAUGCACCUUAU U-3′; anti-miRNA (inhibitor-18a): 5′-CUAUCUGCACUAGAUGCA CCUUA-3′; Cy5-PNA: 5′-Cy5-CTATCTGCACTAGATGCACCTTA-3′; Cy5-LNA: 5′-Cy5-CTATCTG*C*ACT*A*GAT*G*CACCTTA-3′; Cy5-ssDNA: 5′-Cy5-CTATCTGCACTAGATGCACCTTA-3′; single-base mismatched strand: 5′-UAAGGUGCAUC*G*AGUG CAGAUAG-3′; three-base mismatched strand: 5′-UAAGG*A*GCAUCU*C*GUG CA*U* AUAG-3′; non-complementary RNA: 5′-UGGAGUGUGACAAUGGUGU UUG-3′; background calibration strand: 5′-Cy5-AAAAAAAAAAAAA AAA-3′; NH_2-Poly A: 5′-NH_2-AAAAAA-3′; Cy5-Poly A: 5′-Cy5-AAAAAA-3′.

Instrumentation

Laser scanning confocal microscopy (LSCM) images were obtained on a TCS SP5 laser scanning confocal microscope (Leica, Germany). A transmission electron micrograph (TEM) was obtained using a JEM-2100 TEM instrument (JEOL, Japan). Zeta potential analysis was performed on a Zetasizer (Nano-Z, Malvern, UK). Flow cytometric (FCM) analysis was performed on a Coulter FC-500 flow cytometer (Beckman-Coulter, USA). UV-vis absorption spectra were obtained with a UV-3600 UV-vis-NIR spectrophotometer (Shimadzu, Japan). Fluorescence spectra were recorded on a RF-5301PC spectrofluorometer (Shimadzu, Japan). The MTT assay was performed on a microplate reader (680, Bio-Rad, USA). The cell number was determined using a Petroff-Hausser cell counter (USA). The X-ray diffraction (XRD) pattern was recorded on a D8 Advance X-ray diffractometer (Bruker, Germany) using Cu Kα radiation (λ = 1.5418 Å). The X-ray photoelectron spectroscopic (XPS) measurement was performed using an ESCALAB 250 spectrometer (Thermo-VG Scientific, USA) with an ultrahigh vacuum generator.

Cell culture

HepG2, HeLa and HaCaT cells were cultured in Dulbecco's modified Eagle's medium (DMEM, GIBCO), MDA-MB-231 and A549 cells were cultured in L-15 and RPMI-1640 (GIBCO), respectively, and supplemented with 10% fetal calf serum, penicillin (80 U mL^{-1}), and streptomycin (80 μg mL^{-1}) at 37 °C under a humidified atmosphere containing 5% CO_2, while Opti-MEM was used for cell transfection.

Synthesis of CNNS and preparation of the f-CNNS probe

Bulk g-C_3N_4 was prepared by polymerization of melamine molecules at high temperature, and CNNS was prepared by sonicating the bulk g-C_3N_4 in water.[31] The sonicated mixture was first centrifuged at 5000 rpm to remove aggregated bulk g-C_3N_4 particles and obtain the CNNS suspension, which was centrifuged at 15 000 rpm to obtain CNNS. The CNNS was redispersed in ultrapure water to a concentration of 1.5 mg mL^{-1}.

The FA-Poly A was prepared by adding 3.2 mg EDC and 4.8 mg NHS in 7.91 mL pH 6.0 MES containing 6 μM FA. After the mixture was stirred at room temperature for 5 min, 10 μL 2-mercaptoethanol was added to quench the excess EDC. Then, 80 μL 300 μM NH_2-Poly A was added to the mixture and stirred at room temperature for 4 h.[36,41] The concentration of

the obtained FA-Poly A was 3 μM, expressed as the amount of NH_2-Poly A.

The f-CNNS probe was prepared as follows: 70 μL 1.5 mg mL^{-1} CNNS was diluted with 2.86 mL 20 mM pH 7.4 Tris-HCl buffer and sonicated for 5 min to obtain a homogeneous dispersion. Subsequently, 15 μL 10 μM Cy5-PNA was added to the dispersion and stirred for 5 min at room temperature. 50 μL 3 μM fresh FA-Poly A was then added to the mixture and stirred for another 5 min. After the mixture was centrifuged at 15 000 rpm for 20 min, the resulting f-CNNS probe was redispersed in 70 μL 20 mM pH 7.4 Tris-HCl buffer and stored at 4 °C, the concentration of the f-CNNS probe was 1.5 mg mL^{-1}, expressed as the amount of CNNS.

As control, Cy5-LNA or Cy5-ssDNA and folate functionalized CNNS (LNA-CNNS or DNA-CNNS) were prepared as follows: 200 μL 1.5 mg mL^{-1} CNNS was diluted with 2.73 mL 20 mM pH 7.4 Tris-HCl buffer and sonicated for 5 min to obtain a homogeneous dispersion. 15 μL 10 μM Cy5-LNA or Cy5-ssDNA was added to the dispersion and stirred for 5 min at room temperature, and then 50 μL 3 μM fresh FA-Poly A was added to the mixture and stirred for another 5 min. After the mixture was centrifuged at 15 000 rpm for 20 min, the resulting CNNS was redispersed in 200 μL 20 mM pH 7.4 Tris-HCl buffer and stored at 4 °C, the concentration of LNA-CNNS or DNA-CNNS was 1.5 mg mL^{-1}, expressed as the amount of CNNS, respectively. The supernatants were collected to characterize the amounts of Cy5-PNA, LNA and ssDNA loaded on CNNS by FL detection with a standard curve method. The average loading quantity was 1.35, 0.474 and 0.473 nM on 1.0 μg mL^{-1} CNNS, respectively.

The background calibration probe was also prepared with a similar process as the f-CNNS probe using a background calibration strand instead of Cy5-PNA. The folate functionalized CNNS (FA-CNNS) and Cy5-PNA functionalized CNNS (PNA-CNNS) were prepared by mixing the dispersion of CNNS with folate and Cy5-PNA solution with a similar process, respectively. The FA-CNS and FA-GO were also prepared by mixing folate solution with the dispersion of CNS or GO.

MTT assay

1.0×10^4 HepG2, HeLa and MDA-MB-231 cells were seeded in a 96-well plate containing 100 μL Opti-MEM in each well for 12 h. These cells were incubated with 100 μL Opti-MEM as control and 100 μL Opti-MEM containing f-CNNS (10 to 800 μg mL^{-1}), 35 μg mL^{-1} f-CNS or f-GO for 3 h, or 35 μg mL^{-1} f-CNNS probe for 1 to 12 h. 50 μL MTT (1 mg mL^{-1}) was then added to each well. After incubation for 4 h, the media were removed, and 150 μL dimethylsulfoxide was added to solubilize the formed formazan dye. After 15 min, the absorbance of each well was measured at 490 nm. The relative cell viability (%) was calculated by $(A_{test}/A_{control}) \times 100$.

Cell-specific transfection

1.0×10^4 HepG2 cells were cultivated for 12 h in a 35 mm confocal dish. Then the cells were treated with 500 μL Opti-MEM containing 35 μg mL^{-1} FA-CNNS or CNNS for different times. As control, A549 and HaCaT cells were treated with 500 μL Opti-MEM containing 35 μg mL^{-1} FA-CNNS for different times.

To perform the flow cytometric analysis, 1.0×10^5 HepG2 cells were cultivated in a 60 mm culture dish for 12 h and treated with 5 mL Opti-MEM containing a 35 μg mL^{-1} f-CNNS probe or PNA-CNNS for different times. The competitive test was performed by incubating the cells with 5 mL Opti-MEM containing saturated FA for 1 h prior to the transfection with the f-CNNS probe, which saturated the FR sites on the cell surface.

Subcellular localization

The subcellular localization of the f-CNNS probe was observed by confocal microscopy. HepG2 cells were incubated in (1) 35 μg mL^{-1} f-CNNS probe for 3 h and then 1.0 μM Hoechst 333342 for 20 min, (2) 35 μg mL^{-1} f-CNNS probe and then 1.0 μM LysoTracker Green DND-26 for 20 min, and (3) 35 μg mL^{-1} FA-CNNS for 3 h and then 1.0 μM LysoTracker Green DND-26 for 20 min. The Hoechst 333342 was excited at 405 nm to collect the emission from 410 to 480 nm, while LysoTracker DND-26 was excited at 488 nm, and the emission was collected from 500 to 580 nm.

Confocal microscopic analysis of intracellular miRNA

1.0×10^4 HepG2, HeLa or MDA-MB-231 cells were cultivated in a 35 mm confocal dish for 12 h and treated with 500 μL Opti-MEM, or HepG2 cells were treated with 500 μL Opti-MEM containing 50 nM inhibitor-18a, or 5 nM miRNA-18a mimic for 48 h at 37 °C. These cells were then transfected with a 35 μg mL^{-1} f-CNNS probe or a background calibration probe at 37 °C for 3 h, respectively. After washing with PBS, these cells were used to perform confocal imaging analysis for miRNA detection. The signal from the background calibration probe was used to eliminate the background by adjusting the "offset" button of LSCM. The FL intensity was digitized by Leica Application Suite Advanced FL (LAS-AF) software. The mean FL intensity of each sample was obtained from 7 transfected cells.

Flow cytometric analysis of intracellular miRNA

1.0×10^5 HepG2, HeLa or MDA-MB-231 cells were cultivated in a 60 mm culture dish for 12 h and treated with 5 mL Opti-MEM, or HepG2 cells were treated with 5 mL Opti-MEM containing 50 nM inhibitor-18a, or 5 nM miRNA-18a mimic for 48 h at 37 °C. All these cells were then treated with fresh 5 mL Opti-MEM containing a 35 μg mL^{-1} f-CNNS probe for 3 h to perform the flow cytometric analysis. The background calibration probe transfected cells were also collected for background calibration.

RT-PCR analysis of intracellular miRNA

1.0×10^6 HepG2, HeLa or MDA-MB-231 cells were cultivated in a 10 cm culture dish for 12 h and treated with 50 mL Opti-MEM. Meanwhile, 1.0×10^6 HepG2 cells were treated with 50 mL Opti-MEM containing 50 nM inhibitor-18a, or 5 nM miRNA-18a mimic for 48 h at 37 °C. The total RNA of these cells was extracted using RNAiso Plus (Takara Bio Inc.) accord-

ing to the manufacturer's instructions and digested with DNase I, respectively. 1 μg of total RNA was reverse-transcribed to cDNA using a Mir-X miRNA First-Strand Synthesis Kit (Takara Bio Inc.), and the resulting cDNA was subjected to quantitative real-time PCR using a SYBR® Premix Ex Taq II (Takara Bio Inc.) by using a CFX96™ real-time PCR detection system (Bio-Rad), according to the manufacturer's instructions. All reactions were performed in triplicate, and U6 was used as the internal control. An mRQ 3′ primer (miRNA-18a reverse primer), U6 forward primer and U6 reverse primer were included in the Mir-X miRNA First-Strand Synthesis Kit, and a miRNA-specific primer (miRNA-18a forward primer) was also provided by Takara Bio Inc., China, and the primer sequences were verified and reserved by the Takara Bio Inc., China.

Results and discussion

Characterization of the f-CNNS probe

The CNNS was characterized in previous work.[42] After Cy5-PNA was assembled on CNNS, the zeta potential did not change due to the uncharged PNA, while the UV-vis absorption spectrum showed the characteristic peak of Cy5 and remarkable hypochromicity (Fig. S1, ESI†), suggesting that Cy5-PNA was successfully adsorbed on the surface of CNNS.[36] The loading of FA-Poly A on the CNNS surface led to a more negative zeta potential (Fig. S2, ESI†), which confirmed the successful preparation of the f-CNNS probe.

In vitro quenching and recovery of FL emission

The FL quenching ability of CNNS on Cy5 and the release of dye-labeled oligonucleotide from the CNNS surface upon hybridization with complementary miRNA were first examined. With the increasing amount of CNNS added to a Cy5-PNA solution, the FL of Cy5 gradually decreased (Fig. 2A and Fig. S3, ESI†), indicating the quenching effect of CNNS on the FL of Cy5 due to the adsorption of PNA on the CNNS surface, which led to the static electronic communication between Cy5 and CNNS.[36,43] The addition of complementary miRNA into the corresponding mixture led to the recovery of Cy5 FL, and the

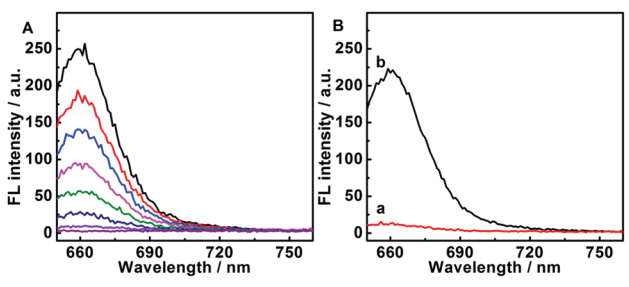

Fig. 2 FL emission spectra of (A) 50 nM Cy5-PNA after incubation with 0, 5, 10, 15, 20, 25, and 35 μg mL^{-1} CNNS at 37 °C for 5 min and 35 μg mL^{-1} CNNS (from top to bottom), and (B) 35 μg mL^{-1} f-CNNS probe (a) after incubation with 250 nM miRNA-18a (b) at 37 °C for 1 h. All measurements are performed in HB.

FL recovery efficiency decreased with the increasing amount of CNNS. Considering the quenching and recovery efficiency of Cy5 FL, the amount of CNNS for 50 nM Cy5-PNA as the optimal conditions for the preparation of the f-CNNS probe was 35 μg mL^{-1}. As control, the FL quenching and recovery of Cy5-LNA and Cy5-ssDNA were also evaluated (Fig. S4, ESI†), the amount of CNNS for the preparation of LNA-CNNS and DNA-CNNS at 50 nM Cy5-LNA and Cy5-ssDNA was 100 μg mL^{-1}, respectively. Cy5-ssDNA and Cy5-LNA required the CNNS amount about three times higher than Cy5-PNA, indicating a higher loading capacity of Cy5-PNA on the CNNS surface than Cy5-LNA and Cy5-ssDNA. This could be attributed to the uncharged backbones of PNA, and the repulsive force between the negatively charged phosphate backbones of ssDNA or LNA and the CNNS surface. Notably, CNNS did not exhibit the obvious FL emission in the examined range (Fig. 2A), indicating that the interference of CNNS with FL detection was negligible.

The f-CNNS probe suspension displayed a significant FL enhancement upon addition of the complementary miRNA-18a (Fig. 2B), indicating the specific recognition of miRNA-18a to Cy5-PNA assembled on the f-CNNS probe, which formed a PNA-miRNA duplex helix to weaken the π–π interaction between the bases and CNNS, and thus led to FL recovery owing to the efficient release of the Cy5-PNA from the probe.

Specificity of the f-CNNS probe

The specific recognition of Cy5-PNA to miRNA-18a was confirmed by examining the change of fluorescence intensity upon incubation of the f-CNNS probe with different sequences. The f-CNNS probe displayed high specificity for discriminating the complementary target from three- and single-base mismatched strands and non-complementary RNA. The increased fluorescence intensities for non-complementary, three- and single-base mismatch RNA were only 0.782%, 18.2% and 28.1% of the complementary target, respectively (Fig. S5, ESI†). As control, the increased fluorescence intensities of LNA- or DNA-CNNS for non-complementary, three- and single-base mismatch RNA were 1.43% or 1.96%, 21.8% or 25.5%, and 32.2% or 36.4% of the complementary target (Fig. S5, ESI†), respectively, indicating higher sequence specificity of the f-CNNS probe than its counterparts LNA-CNNS and DNA-CNNS. This could be attributed to high selectivity and specificity of PNA toward target miRNA.[34] Thus, the proposed system possessed a high signal-to-noise ratio for detection of target miRNA-18a.

The effect of pH on the stability of the f-CNNS probe was also evaluated. The f-CNNS probe taken up by cells experienced an increasingly acidic environment as it progressed through the endocytic pathway due to the pH change from 4.7 to 8.0.[44] The LNA-CNNS, DNA-CNNS and f-CNNS probes showed a slight fluorescence change at pH ranging from 4.0 to 8.0 (Fig. S6, ESI†), indicating that they were stable during the endocytic pathway for intracellular transport. The fluorescence change of the f-CNNS probe was lower than the LNA-CNNS

and DNA-CNNS, demonstrating the lower background signal of the f-CNNS probe in a complex biological environment. This could also be attributed to the uncharged characteristic of PNA, and the repulsive force between the negatively charged phosphate backbones of ssDNA or LNA and the CNNS surface.

Protection properties and cytotoxicity of CNNS

Oligonucleotides are susceptible to degradation by cellular nucleases during delivery into the cells. Therefore, an efficient delivery vector should protect the cargo against nuclease digestion and SSB interaction during prolonged transport. Herein, the ability of CNNS to protect the oligonucleotides from nuclease cleavage and interfering proteins was studied. The f-CNNS probe, LNA-CNNS and DNA-CNNS suspensions presented low fluorescence intensity. After incubation with miRNA-18a, all these suspensions showed a sharp increase of Cy5 FL (Fig. 3), respectively. However, after they were incubated with 250 nM SSB or 1.0 U DNase I, the fluorescence intensity increased by only 4.76% or 5.29%, 7.16% or 7.51% and 10.6% or 12.1% of that with the complementary miRNA-18a, respectively. Thus, CNNS could well resist DNase I cleavage and the SSB interaction. The protection could be attributed to the shielding from the CNNS or the conformational change of nucleic acid strands when adsorbed on the CNNS surface.[45]

To exactly evaluate the cytotoxicity of a gene carrier, HepG2 cells were treated with FA-CNNS from 10 to 800 μg mL^{-1} to perform the MTT assay, which exhibited the viability from 99.1% to 91.1% (Fig. S7A, ESI†), suggesting that CNNS possessed low cytotoxicity. The viability of cells transfected with FA-CNNS was even higher than those transfected with FA-CNS and FA-GO (Fig. S7B, ESI†), indicating lower cytotoxicity of the CNNS than CNS and GO. The low cytotoxicity of the f-CNNS probe was also demonstrated by treating HepG2, HeLa and MDA-MB-231 cells with 35 μg mL^{-1} f-CNNS probe for 1 to 12 h, which exhibited the viability from 99.3% to 93.9%, 99.6% to 94.2%, and 99.5% to 93.7%, respectively (Fig. S8 and S9, ESI†). The efficient protection properties, good stability and low cytotoxicity led to promising applications of the probe in *in situ* monitoring of intracellular biomolecules.

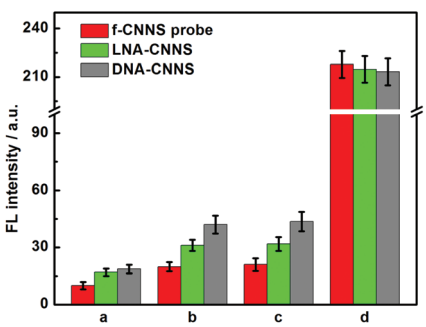

Fig. 3 FL intensity of the f-CNNS probe, LNA-CNNS and DNA-CNNS (a) after incubation with 250 nM SSB (b), 1.0 U DNase I (c) and 250 nM miRNA-18a (d) at 37 °C for 1 h. The concentrations of the f-CNNS probe, LNA-CNNS and DNA-CNNS were 35, 100 and 100 μg mL^{-1}, respectively. All measurements are performed in HB.

Evaluation of cell-specific delivery

Cell-specific delivery can limit the side effects from nonspecific delivery and reduce the quantity of the gene probe needed. This work used FA to achieve the cell-specific delivery of the f-CNNS probe into HepG2 cells by its recognition to a folate receptor overexpressed on the cell membrane. The receptor-mediated endocytosis was thus evaluated, and the cell-specific transfection of FA-CNNS in living cells could be monitored by the FL of CNNS. As shown in Fig. 4, with the increasing incubation time of HepG2 cells with the FA-CNNS suspension, the transfected cells showed increasing FL of CNNS (column A), indicating the increasing uptake of FA-CNNS. However, the HepG2 cells transfected with CNNS showed low FL (column B). Thus, the presence of FA on CNNS was necessary for cell-specific transfection due to the presence of a folate receptor (FR) overexpressed on cancer cells. The FR-mediated endocytosis of FA-CNNS could be confirmed with A549 cells (FR-negative cells, column C) and HaCaT cells (non-cancerous cells, column D), which also showed very low FL of CNNS (Fig. S10, ESI†).

To further confirm the FR-mediated endocytosis of the f-CNNS probe, a competitive binding test with free FA and the transfection of PNA-CNNS in the absence of FA were carried out. With the increasing incubation time of the f-CNNS probe, the HepG2 cells showed increasing FL (Fig. S11a, ESI†), indicating the increased uptake of the f-CNNS probe. In contrast, after HepG2 cells were firstly treated with FA to saturate the FR sites on the cell surface, the cells transfected with the f-CNNS probe showed very low FL due to the occupancy of FRs by free FA (Fig. S11b, ESI†), which reduced the FR-mediated endocytosis.[46] In the absence of FA, the transfection of PNA-CNNS also

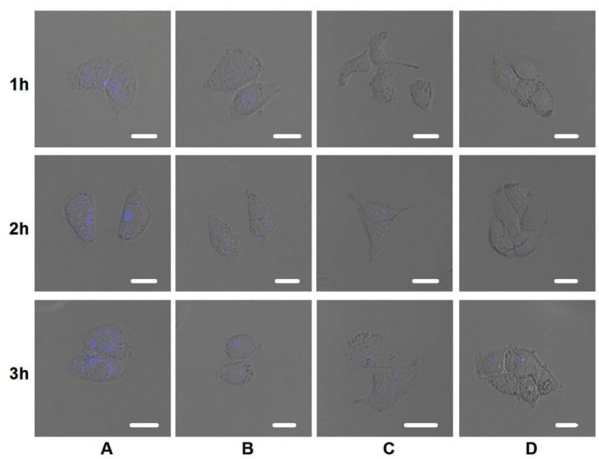

Fig. 4 Confocal microscopy images of HepG2 cells transfected with 35 μg mL^{-1} (A) FA-CNNS, (B) CNNS, (C) A549 and (D) HaCaT cells transfected with 35 μg mL^{-1} FA-CNNS at 37 °C for 1, 2 and 3 h. Scale bars: 20 μm.

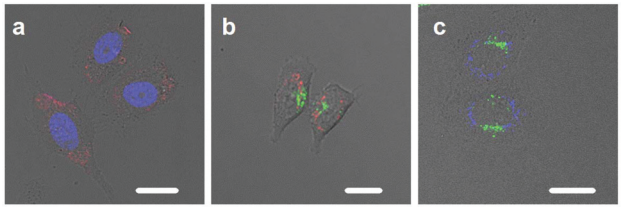

Fig. 5 Confocal microscopy images of HepG2 cells transfected with 35 μg mL^{-1} f-CNNS probe for 3 h and then 1.0 μM Hoechst 333342 for 20 min (a), 35 μg mL^{-1} f-CNNS probe (b) and FA-CNNS (c) for 3 h and then 1.0 μM LysoTracker Green DND-26 for 20 min at 37 °C. Scale bars: 20 μm.

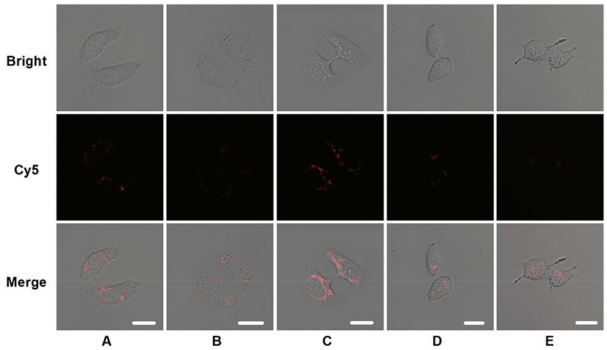

Fig. 6 Confocal microscopy images of HepG2 cells (A), HepG2 cells treated with 50 nM inhibitor-18a (B), 5 nM miRNA-18a mimic (C) for 48 h, HeLa (D) and MDA-MB-231 (E) cells, and then transfected with 35 μg mL^{-1} f-CNNS probe at 37 °C for 3 h. Scale bars: 20 μm.

showed little uptake (Fig. S11c, ESI†). These results confirmed that the up-take of the f-CNNS probe was FR-mediated.

Subcellular localization of the f-CNNS probe

After cellular internalization, the f-CNNS probe would be delivered to early endosomes, followed by the movement to late endosomes/lysosomes.[47] Thus, the successful endosomal escape of the probe was a critical requirement for miRNA-18a detection. Colocalization experiments were performed to demonstrate the endosomal escape of the f-CNNS probe. After HepG2 cells were incubated with the f-CNNS probe and Hoechst 333342, the cells showed strong Cy5 FL in cytoplasm due to the hybridization of Cy5-PNA on the probe with miRNA-18a (Fig. 5a), indicating the presence of miRNA and the f-CNNS probe in the cytoplasm. The f-CNNS probe and Lysotracker Green DND-26 transfected HepG2 cells showed strong Cy5 FL without colocalization with endocytic vesicles in the cytoplasm (Fig. 5b), indicating that the f-CNNS probe successfully escaped from endocytic vesicles to recognize miRNA-18a in the cytoplasm.[47,48] The FA-CNNS and Lysotracker Green DND-26 transfected HepG2 cells also showed strong CNNS FL without colocalization with endocytic vesicles in the cytoplasm (Fig. 5c), indicating the successful endosomal escape and efficient cytoplasmic diffusion of the f-CNNS probe.

Detection of intracellular miRNA

To investigate the capability of the f-CNNS probe for monitoring intracellular miRNA, the incubation time and amount of the f-CNNS probe for HepG2 cells were optimized to be 3 h and 35 μg mL^{-1} by confocal microscopy (Fig. S12, ESI†), and the optimal conditions were also suitable to HeLa and MDA-MB-231 cells (Fig. S13, ESI†). To obtain the real samples, the HepG2 cells were incubated with an miRNA inhibitor or miRNA-18a mimic[49] to induce different levels of miRNA, then incubated with the f-CNNS probe and subsequently analyzed by confocal microscopy.

The cells exhibited a strong FL signal of Cy5 (Fig. 6A), indicating high levels of miRNA-18a in HepG2 cells.[50] After HepG2 cells were incubated with inhibitor-18a (Fig. 6B), the miRNA-18a levels showed 46.2% down-regulation (Fig. S14, ESI†). When HepG2 cells were incubated with miRNA-18a mimic (Fig. 6C), the miRNA-18a level showed 135.5% up-regulation (Fig. S14, ESI†). In parallel monitoring, HeLa and MDA-MB-231 cells showed 73.9% and 29.6% (Fig. 6D and E) of the miRNA-18a expression levels of HepG2 cells. Thus, the proposed method could be used for *in situ* monitoring the dynamic changes of intracellular miRNA.

Flow cytometric analysis of intracellular miRNA was performed to confirm the detection results (Fig. S15, ESI†). The miRNA-18a levels of HepG2 cells incubated with inhibitor-18a showed 48.7% down-regulation. When HepG2 cells were incubated with miRNA-18a mimic, the miRNA-18a level showed 132.0% up-regulation. HeLa and MDA-MB-231 cells showed 75.8% and 31.8% of the miRNA-18a expression level in HepG2 cells, respectively.

To further confirm the detection results, quantitative real-time PCR analysis was used to detect the miRNA-18a levels. After HepG2 cells were incubated with inhibitor-18a, miRNA-18a showed 47.3% down-regulation, while the incubation with miRNA-18a mimic led to 142.8% up-regulation of the miRNA-18a level (Fig. S16, ESI†). HeLa and MDA-MB-231 cells showed 68.9% and 27.5% of the miRNA-18a level expressed in HepG2 cells, respectively. These results were in good agreement with those obtained with the proposed method, indicating good validation of the proposed method.

Conclusions

This work successfully assembles Cy5-PNA and FA on the CNNS surface to design an f-CNNS probe for target-cell-specific monitoring of intracellular miRNA. The CNNS shows low cytotoxicity and a strong quenching ability on Cy5 FL, which can be recovered upon the specific recognition of the Cy5-PNA to miRNA due to the release of the formed PNA-miRNA duplex helix from the CNNS surface. The high fluorescence recovery efficiency, low fluorescence background and good gene protection properties of CNNS, and the uncharged characteristic of PNA, which strengthens its interaction with the CNNS surface,

lead to high sensitivity and specificity of the suggested method for *in situ* monitoring of intracellular miRNA. The designed sensing strategy realizes the detection of miRNA in living cells. By virtue of these advantages, the proposed strategy implies the potential for biomedical research and clinical diagnostics.

Acknowledgements

This work was financially supported by the National Natural Science Foundation of China (21121091, 21135002, 91413118) and Priority development areas of The National Research Foundation for the Doctoral Program of Higher Education of China (20130091130005).

References

1 R. H. Plasterk, *Cell*, 2006, **124**, 877–881.
2 M. V. Joglekar, V. M. Joglekar and A. A. Hardikar, *Gene Expression Patterns*, 2009, **9**, 109–113.
3 Y. L. Wang, D. N. Keys, J. K. Au-Young and C. F. Chen, *J. Cell Physiol.*, 2009, **218**, 251–255.
4 J. Brennecke, D. R. Hipfner, A. Stark, R. B. Russell and S. M. Cohen, *Cell*, 2003, **113**, 5–36.
5 N. Kosaka, H. Iguchi and T. Ochiya, *Cancer Sci.*, 2010, **101**, 2087–2092.
6 J. Jiang, E. J. Lee, Y. Gusev and T. D. Schmittgen, *Nucleic Acids Res.*, 2005, **33**, 5394–5403.
7 M. A. Lindsay, *Trends Immunol.*, 2008, **29**, 343–351.
8 B. R. Cullen, *Genes Dev.*, 2011, **25**, 1881–1894.
9 S. M. Johnson, H. Grosshans, J. Shingara, M. Byrom, R. Jarvis, A. Cheng, E. Labourier, K. L. Reinert, D. Brown and F. J. Slack, *Cell*, 2005, **120**, 635–647.
10 C. E. Stahlhut-Espinosa and F. J. Slack, *J. Biol. Med.*, 2006, **79**, 131–140.
11 H. F. Dong, J. P. Lei, L. Ding, Y. Q. Wen, H. X. Ju and X. J. Zhang, *Chem. Rev.*, 2013, **113**, 6207–6233.
12 N. Kosaka, H. Iguchi and T. Ochiya, *Cancer Sci.*, 2010, **101**, 2087–2092.
13 H. Grosshans and W. Filipowicz, *Nature*, 2008, **451**, 414–416.
14 A. Gupta, J. J. Gartner, P. Sethupathy, A. G. Hatzigeorgiou and N. W. Fraser, *Nature*, 2006, **442**, 82–85.
15 J. Li, B. Yao, H. Huang, Z. Wang, C. H. Sun, Y. Fan, Q. Chang, S. L. Li, X. Wang and J. Z. Xi, *Anal. Chem.*, 2009, **81**, 5446–5451.
16 C. Chen, D. A. Ridzon, A. J. Broomer, Z. Zhou, D. H. Lee, J. T. Nguyen, M. Barbisin, N. L. Xu, V. R. Mahuvakar, M. R. Andersen, K. Q. Lao, K. J. Livak and K. J. Guegler, *Nucleic Acids Res.*, 2005, **33**, e179.
17 G. S. Pall, C. Codony-Servat, C. J. Byrne, L. Ritchie and A. Hamilton, *Nucleic Acids Res.*, 2007, **35**, e60.
18 S. W. Kim, Z. Li, P. S. Moore, A. P. Monaghan, Y. Chang, M. Nichols and B. John, *Nucleic Acids Res.*, 2010, **38**, e98.
19 P. T. Nelson, D. A. Baldwin, L. M. Scearce, J. C. Oberholtzer, J. W. Tobias and Z. Mourelatos, *Nat. Methods*, 2004, **1**, 155–161.
20 H. F. Dong, L. Ding, F. Yan, H. X. Ji and H. X. Ju, *Biomaterials*, 2011, **32**, 3875–3882.
21 H. F. Dong, J. P. Lei, H. X. Ju, F. Zhi, H. Wang, W. J. Guo, Z. Zhu and F. Yan, *Angew. Chem., Int. Ed.*, 2012, **51**, 4607–4612.
22 R. C. Qian, L. Ding and H. X. Ju, *J. Am. Chem. Soc.*, 2013, **135**, 13282–13285.
23 R. C. Qian, L. Ding, L. W. Yan, M. F. Lin and H. X. Ju, *J. Am. Chem. Soc.*, 2014, **136**, 8205–8208.
24 S. J. He, B. Song, D. Li, C. F. Zhu, W. P. Qi, Y. Q. Wen, L. H. Wang, S. P. Song, H. P. Fang and C. H. Fan, *Adv. Funct. Mater.*, 2010, **20**, 453–459.
25 S. S. Chou, M. De, J. Luo, V. M. Rotello, J. Huang and V. P. Dravid, *J. Am. Chem. Soc.*, 2012, **134**, 16725–16733.
26 Y. Wang, Z. H. Li, D. H. Hu, C. T. Lin, J. H. Li and Y. H. Lin, *J. Am. Chem. Soc.*, 2010, **132**, 9274–9276.
27 Y. Zheng, Y. Jiao, M. Jaroniec, Y. G. Jin and S. Z. Qiao, *Small*, 2012, **8**, 3550–3566.
28 Y. Wang, X. C. Wang and M. Antonietti, *Angew. Chem., Int. Ed.*, 2012, **51**, 68–69.
29 C. M. Cheng, Y. Huang, X. Q. Tian, B. Z. Zheng, Y. Li, H. Y. Yuan, D. Xiao, S. P. Xie and M. M. F. Choi, *Anal. Chem.*, 2012, **84**, 4754–4759.
30 C. M. Cheng, Y. Huang, J. Wang, B. Z. Zheng, H. Y. Yuan and D. Xiao, *Anal. Chem.*, 2013, **85**, 2601–2605.
31 X. D. Zhang, X. Xie, H. Wang, J. J. Zhang, B. C. Pan and Y. Xie, *J. Am. Chem. Soc.*, 2013, **135**, 18–21.
32 S. R. Ryoo, J. Lee, J. Yeo, H. K. Na, Y. K. Kim, H. Jang, J. H. Lee, S. W. Han, Y. Lee, V. N. Kim and D. H. Min, *ACS Nano*, 2013, **7**, 5882–5891.
33 M. Egholm, O. Buchardt, P. E. Nielsen and R. H. Berg, *J. Am. Chem. Soc.*, 1992, **114**, 1895–1897.
34 M. Egholm, O. Buchardt, L. Christensen, C. Behrens, S. M. Freier, D. A. Driver, R. H. Berg, S. K. Kim, B. Norden and P. E. Nielsen, *Nature*, 1993, **365**, 566–568.
35 B. S. Gaylord, M. R. Massie, S. C. Feinstein and G. C. Bazan, *Proc. Natl. Acad. Sci. U. S. A.*, 2005, **102**, 34–39.
36 Q. B. Wang, W. Wang, J. P. Lei, N. Xu, F. L. Gao and H. X. Ju, *Anal. Chem.*, 2013, **85**, 12182–12188.
37 C. H. Lu, H. H. Yang, C. L. Zhu, X. Chen and G. N. Chen, *Angew. Chem., Int. Ed.*, 2009, **121**, 4879–4881.
38 K. Kogure, R. Moriguchi, K. Sasaki, M. Ueno, S. Futaki and H. Harashima, *J. Controlled Release*, 2004, **98**, 317–323.
39 C. P. Leamon, M. A. Parker, I. R. Vlahov, L. C. Xu, J. A. Reddy, M. Vetzel and N. Douglas, *Bioconjugate Chem.*, 2002, **13**, 1200–1210.
40 X. M. Sun and Y. D. Li, *Angew. Chem., Int. Ed.*, 2004, **43**, 597–601.
41 E. Heister, V. Neves, C. Tîlmaciu, K. Lipert, V. S. Beltrán, H. M. Coley, S. R. P. Silva and J. McFadden, *Carbon*, 2009, **47**, 2152–2160.
42 X. J. Liao, Q. B. Wang and H. X. Ju, *Chem. Commun.*, 2014, **50**, 13604–13607.

43 S. A. E. Marras, F. R. Kramer and S. Tyagi, *Nucleic Acids Res.*, 2002, **30**, e122.
44 J. R. Casey, S. Grinstein and J. Orlowski, *Nat. Rev. Mol. Cell Biol.*, 2010, **11**, 50–61.
45 Y. R. Wu, J. A. Phillips, H. P. Liu, R. H. Yang and W. H. Tan, *ACS Nano*, 2008, **2**, 2023–2028.
46 D. J. Bharali, D. W. Lucey, H. Jayakumar, H. E. Pudavar and P. N. Prasad, *J. Am. Chem. Soc.*, 2005, **127**, 11364–11371.
47 A. K. Varkouhi, M. Scholte, G. Storm and H. J. Haisma, *J. Controlled Release*, 2011, **150**, 220–228.
48 M. Huang, C. W. Fong, E. Khor and L. Y. Lim, *J. Controlled Release*, 2005, **106**, 391–406.
49 J. Kota, R. R. Chivukula, K. A. O'Donnell, E. A. Wentzel, C. L. Montgomery, H. W. Hwang, T. C. Chang, P. Vivekanandan, M. Torbenson, K. R. Clark, J. R. Mendell and J. T. Mendell, *Cell*, 2009, **137**, 1005–1017.
50 Y. Murakami, T. Yasuda, K. Saigo, T. Urashima, H. Toyoda, T. Okanoue and K. Shimotohno, *Oncogene*, 2006, **25**, 2537–2545.